ChemPhysChem

Supporting Information

In situ Surface Charge Density Visualization of Self-assembled DNA Nanostructures after Ion Exchange

Steffan Møller Sønderskov, Lasse Hyldgaard Klausen, Sebastian Amland Skaanvik, Xiaojun Han,* and Mingdong Dong*

Supporting Information Figure 1

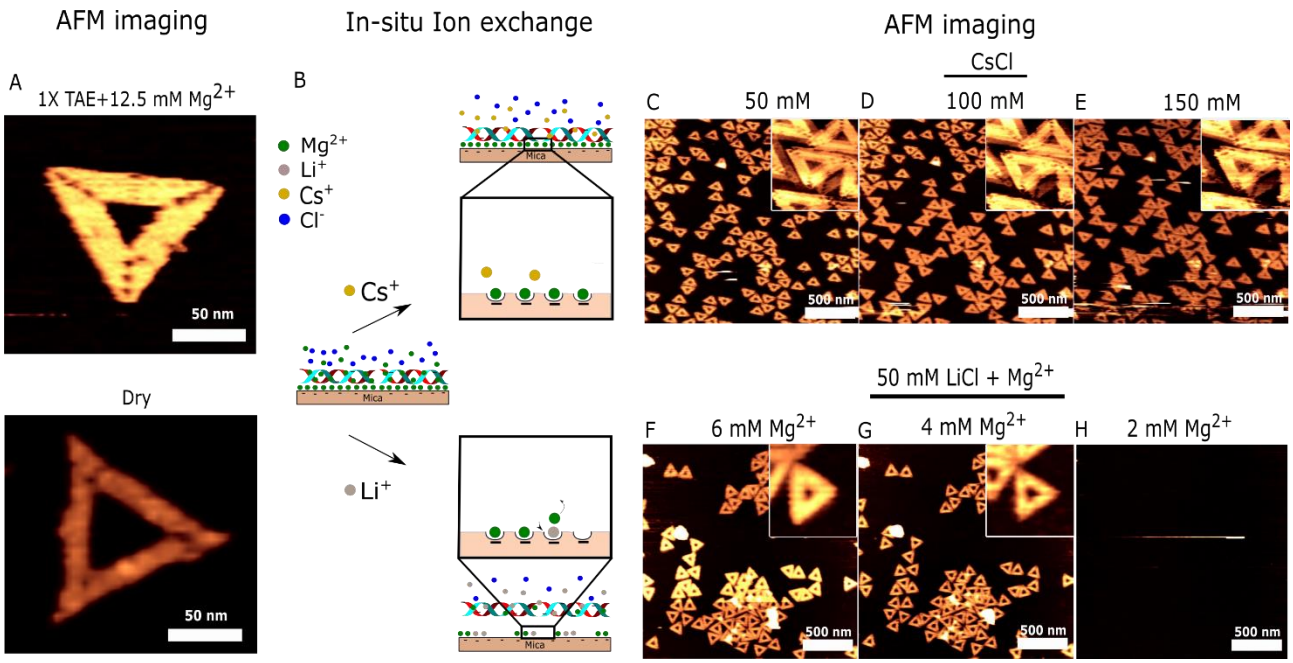

Figure S1. (A) AFM image of DNA origami in standard folding buffer and in dry. *In situ* ion exchange with 50 (C), 100 (D) and 150 (E) mM CsCl and 50/6 (F), 50,4 (G) and 50/2 (H) mM LiCl/Mg^{2+}.

Supporting Information Figure 2

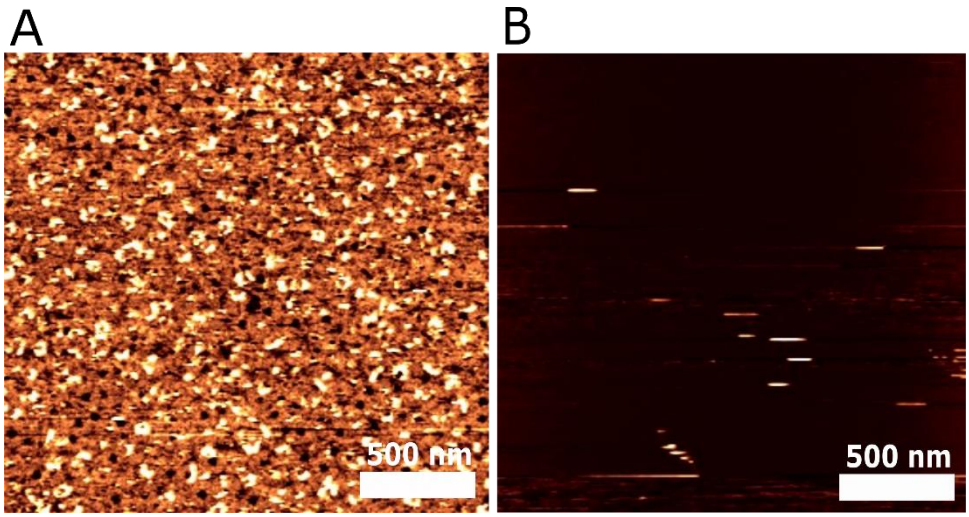

Figure S2. (A) AFM image of a fully covered mica surface with DNA origami. (B) Mica surface where DNA origami has been fully desorbed after adding 50 mM NaCl

Supporting Information Figure 3

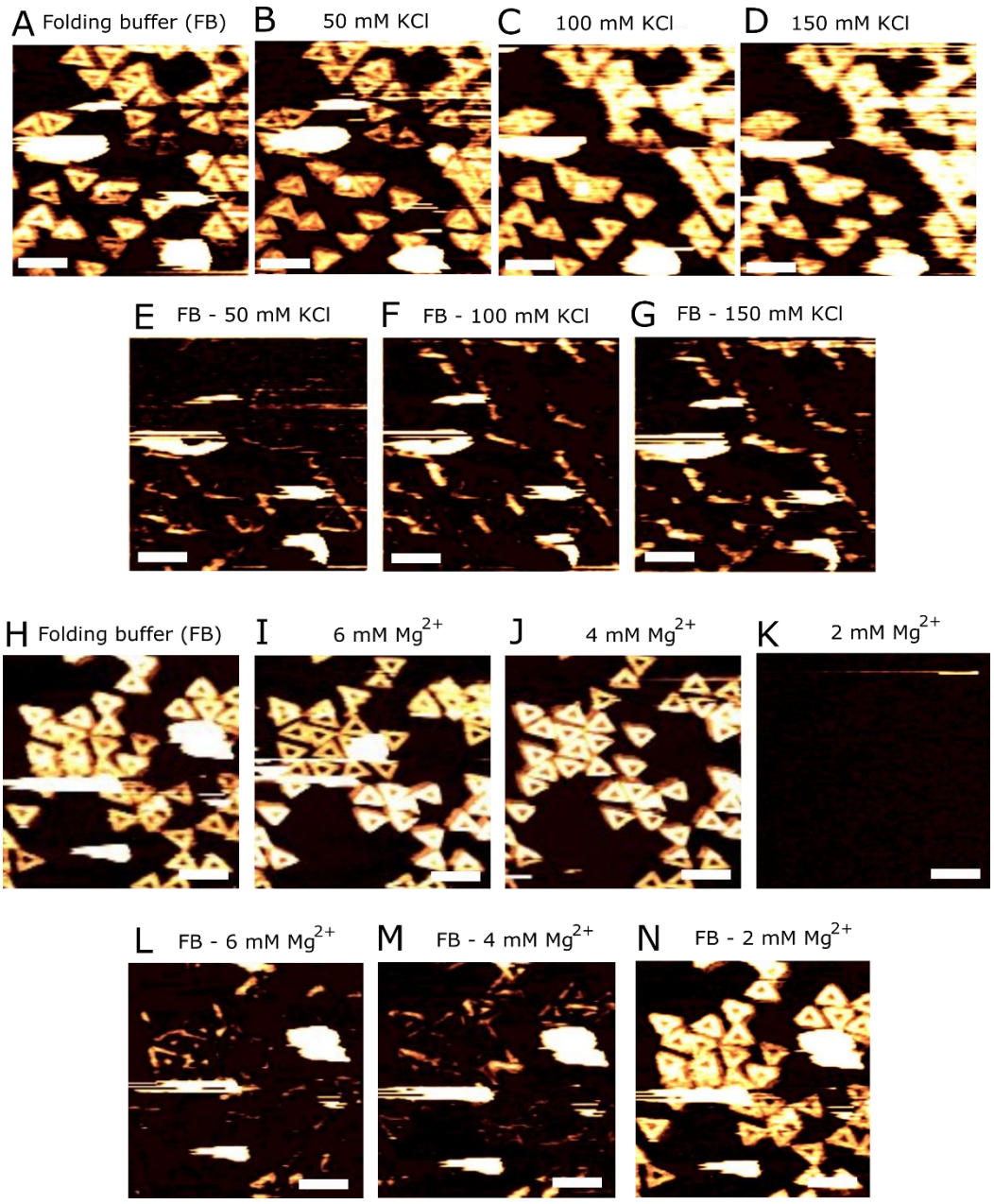

Figure S3. Diffusion study of DNA origami after buffer exchange. (A) AFM image of DNA origami in folding buffer (FB) before ion exchange experiments. AFM images after liquid exchange with 50 mM KCl (B), 100 mM KCl (C) and 150 mM KCl (D). (E, F, G) AFM images **B, C** and **D** respectively are overlaid onto AFM image **A** and afterwards subtracted. (H) AFM image of DNA origami in folding buffer (FB) before ion exchange experiments. AFM images after liquid exchange with 50 mM NaCl + 6 mM Mg^{2+} (I), 50 mM NaCl + 4 mM Mg^{2+}(J) and 50 mM NaCl + 2 mM Mg^{2+}(K). (L, M, N) AFM images are overlaid onto AFM image **H** and afterwards subtracted. Scale bar is 200 nm.

Supporting Information Figure 4

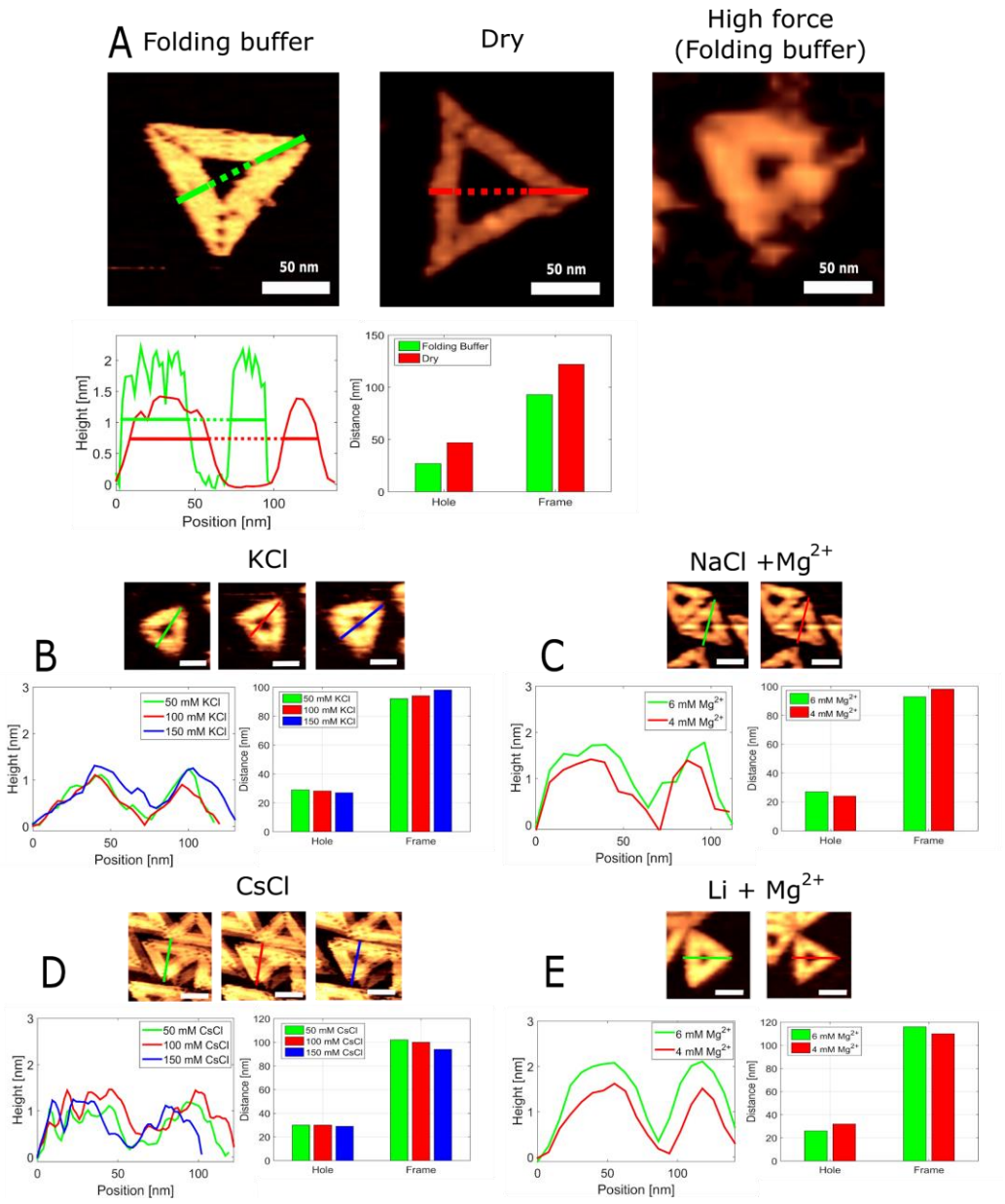

Figure S4. Morphological study of DNA origami after buffer exchange. (A) AFM images comparing the morphology of DNA origami in folding buffer, in dry and under high cantilever force. Morphological analysis is also performed for DNA origami in KCl (B), NaCl + Mg^{2+} (C), CsCl (D) and LiCl + Mg^{2+} (E). Scale Bar is 50 nm.

Supporting Information Figure 5

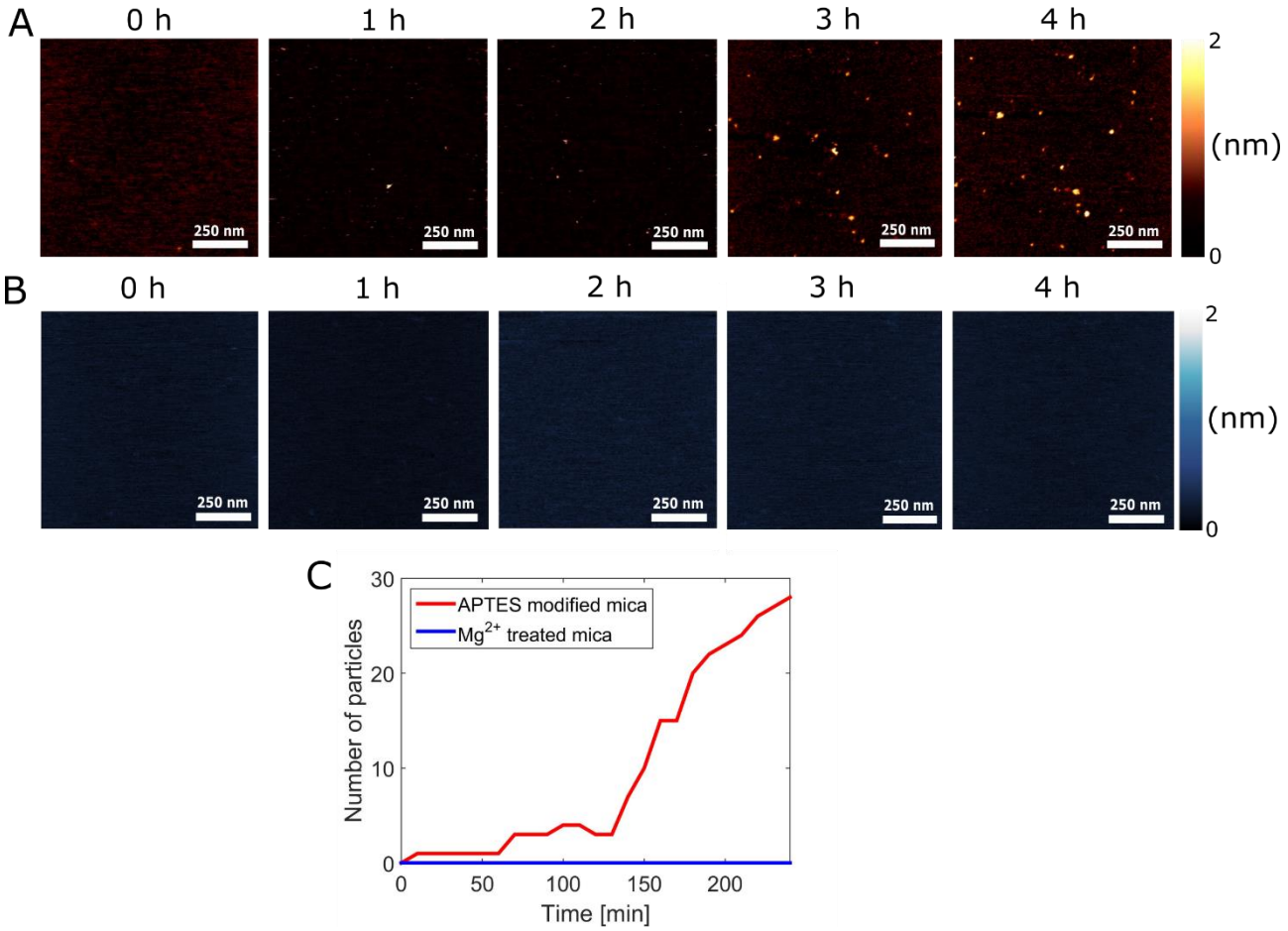

Figure S5. Time-lapse liquid AFM imaging of APTES modified mica surface and Mg^{2+} treated mica (A) Time-lapse liquid AFM images over a period of 4 hours showing clear particle formation on an APTES modified mica surface. (B) Control: Time-lapse liquid AFM imaging over a period of 4 hours on Mg^{2+} treated mica showing no particle formation. (C) Number of countable particles at different time-steps. Particle threshold is 0.5 nm.

Supporting Information Figure 6

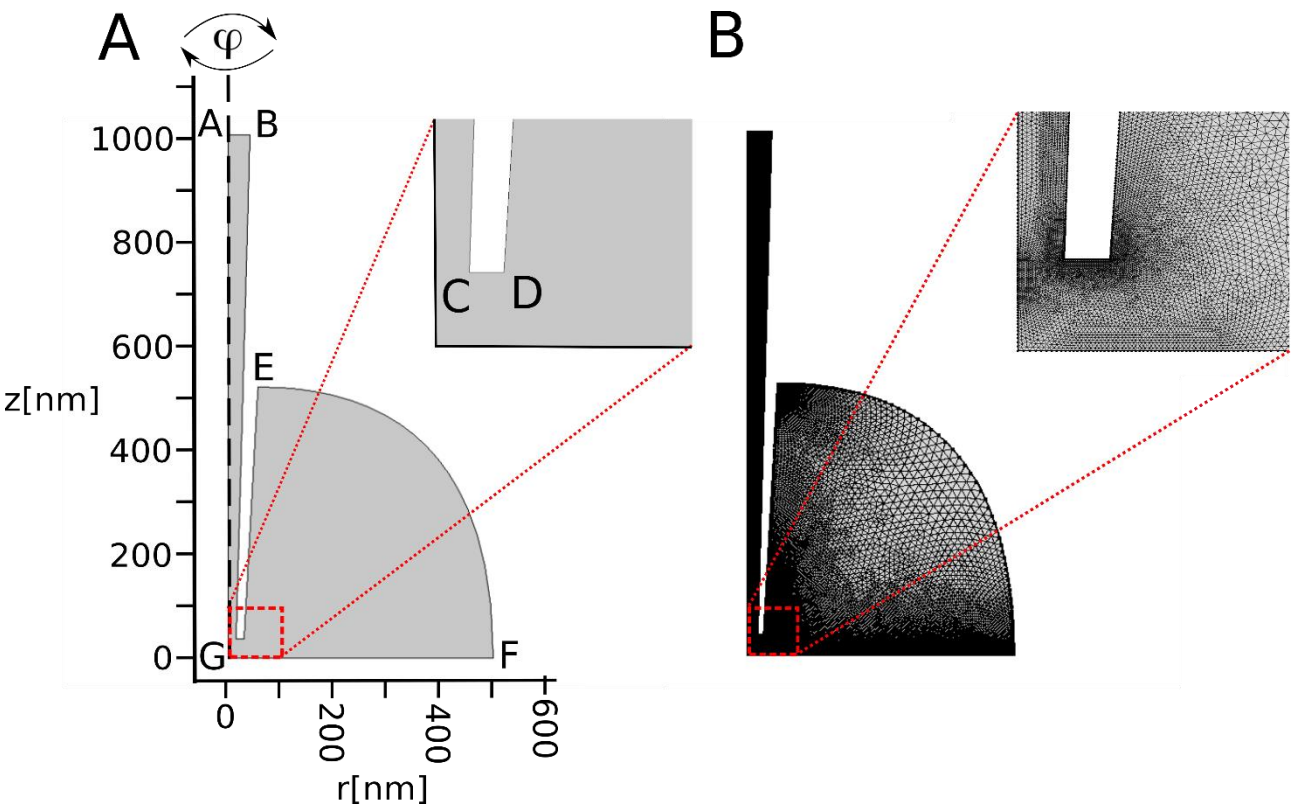

SFigure S6. Finite-element geometry (A) 2D view of the pipette geometry constructed for finite-element analysis. Rotational symmetry was used to minimize computational costs. The grey area represents the electrolyte solution, while the boundaries (between letters A to G) are described in Supplementary Table 2. (B) A triangular mesh model was used for the simulations

Supporting Information Figure 7

The technique of quantitative surface conductivity microscopy (QSCM) allows conversion of the height difference between ±100 mV at 99 % current ($\Delta h_{99\%}$) into SCD. The relation between $\Delta h_{99\%}$ and SCD is: $\Delta h_{99\%}$ = -1.24nm-164.13nm C^{-1} m^2 • SCD in 150 mM NaCl and $\Delta h_{99\%}$ = -0.62nm-168.05nm C^{-1} m^2 • SCD in 150 mM KCl.

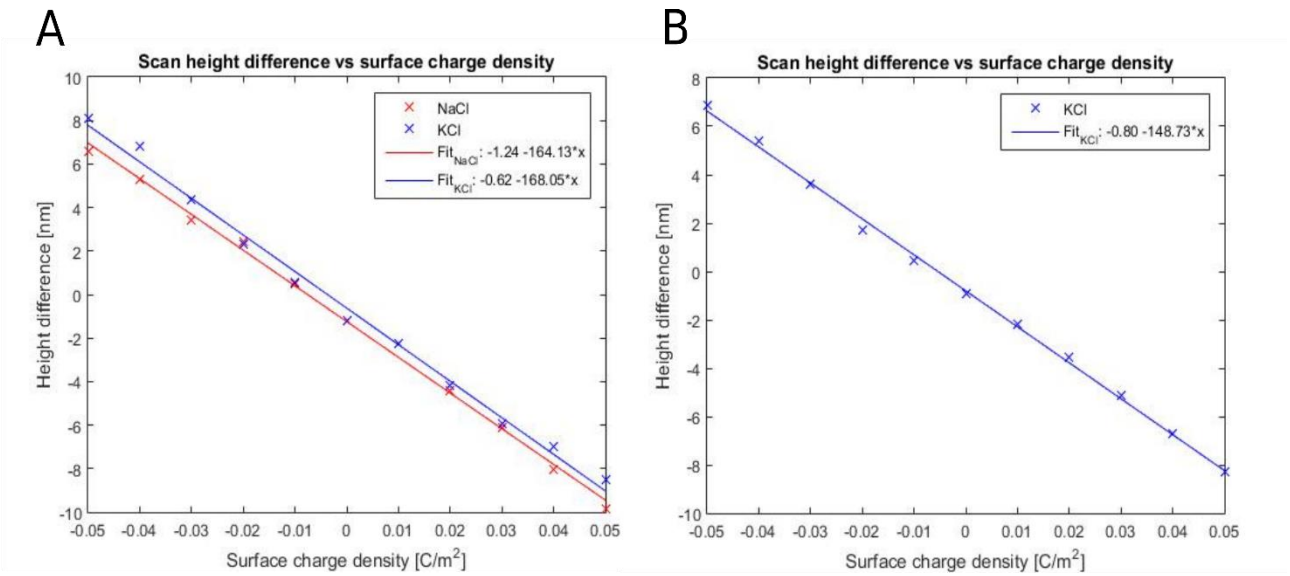

Figure S7. Relation between sample SCD and pipette height difference at 99 % current. Fits were performed on data obtained from finite-element analysis. Pipettes with inner radius of 18.9 nm (A) and 32.6 nm (B) and half angle of 3° were used throughout the simulation. The dimensions were estimated based on the free current and light microscopy imaging

Supporting Information Figure 8

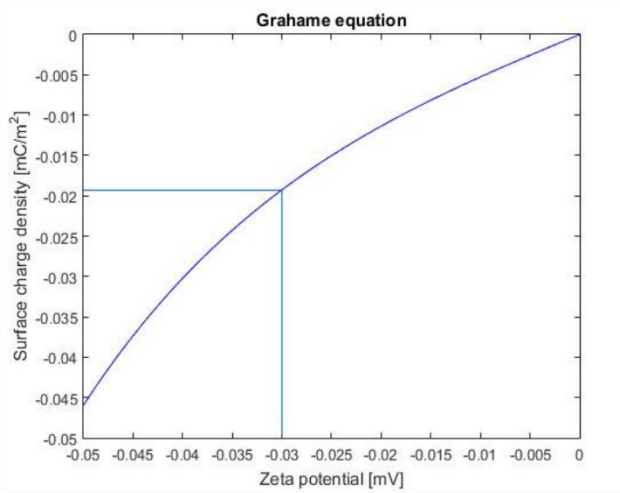

Figure S8. Grahame equation applied to calculate the SCD based on experimental measurement of the zeta potential. The equation was solved based on the electrolyte solution containing 12.5 mM of divalent ions.

Supporting Information Table 1

	Initial attachment	Diffusion/continued attachment				
Literature	Mg^{2+}	Mg^{2+}	Li^{+}	Na^{+}	K^{+}	Cs^{+}
A. A. Rafat, T. Pirzer, M. B. Scheible, A. Kostina, F. C. Simmel, Angewandte Chemie International Edition 2014, 53, 7665–7668	✓ (12.5 mM)	✓ (12.5 mM)	✗	✓ (100-400 mM)	✗	✗
S. Woo, P. W. K. Rothemund, Nature Communications 2014, 5, 4889	✓ (12.5 mM)	✓ (0-12.5 mM)	✗	✓ (0-1.19M)	✗	✗
C. Kielar, S. Ramakrishnan, S. Fricke, G. Grundmeier, A. Keller, ACS Applied Materials & Interfaces 2018, 10, 44844–44853	✓ (10 mM)	✓ (10 mM)	✗	✓ (0-100 mM)	✗	✗
Current study	✓ (12.5 mM)	✓ (2-6 mM)	✓ (50 mM)	✓ (50 mM)	✓ (50-150 mM)	✓ (50-150 mM)

Table S1. Comparison with selected literature examining ionic species for initial attachment and continued attachment/ diffusion of DNA origami.

Supporting Information Table 2

Boundary	Description	Ion flow (NP)	Potential (P)
AB	Pipette top / electrode	Reservoir: $c_i=c$	Electrode: $V=V_0$
BC	Pipette inner wall	Isolating: $n \cdot N_i=0$	Surface charge: $\nabla V=-\sigma_p/\varepsilon_0\varepsilon$
CD	Pipette tip	Isolating: $n \cdot N_i=0$	Surface charge: $\nabla V=-\sigma_p/\varepsilon_0\varepsilon$
DE	Pipette outer wall	Isolating: $n \cdot N_i=0$	Surface charge: $\nabla V=-\sigma_p/\varepsilon_0\varepsilon$
EF	Water bath / electrode	Reservoir: $c_i=c$	Electrode: $V=0$
FG	Sample surface	Isolating: $n \cdot N_i=0$	Surface charge: $\nabla V=-\sigma_s/\varepsilon_0\varepsilon$
GA	Symmetry axis	Symmetry	Symmetry

Table S2. Boundary conditions applied for simulations. The boundaries (between letters A to G) are shown in Supplementary Figure 6.

Supplementary note 1

The measured scanning height was correlated to surface charges using Poisson-Nernst-Planck finite element simulations. A schematic of the simulation setup and formed finite element setup is shown in Supplementary Figure 3. Simulations were performed by simultaneously solving the Poisson equation, , $\nabla^2 V = \frac{-F}{\varepsilon\varepsilon_0}\sum_i z_i c_i$, and the Nernst Planck equation, $\nabla\left(-D_i\nabla c_i - \frac{D_i z_i c_i F}{RT}\nabla V\right) = 0$. V is the electrostatic potential, ε the relative permittivity, c_i the concentration and z_i the charge of ion i, F is the Faraday constant and ε_0 is the vacuum permittivity. D_i is the diffusion constant of ion i, R is the gas constant and T the temperature. The ionic current was calculated as the integral over the total charge passing a boundary spanning the inside of the nanopipette:

$$I = \int_0^A F \sum_i z_i N_i \, dl$$

Supplementary note 2

The inner radius of the nanopipettes were estimated by comparison to finite element simulations in COMSOL based on the measured ionic current. The following formula was used to correlate the measured ionic current (I_{tot}) to the simulated ionic current when taking into account the resistance of the areas outside the finite element simulation box:

$$I_{tot} = \frac{V}{R_{tot}} = \frac{V}{R_{sim} + R_{xtra}} = \frac{1}{\frac{1}{I_{sim}} + \frac{R_{xtra}}{V}} = \frac{1}{\frac{1}{I_{sim}} + \frac{\rho}{V\pi}\left(\frac{1}{2W} + \frac{1}{tan\,\theta\, L}\right)}$$

Supplementary note 3

The theoretical SCD of the two-dimensional (2D) triangular DNA origami frame is calculated based on the intrinsic charge of DNA and the surface area of the structure. Total amount of charge is calculated based on the number of nucleotides in the M13 plasmid (7249) and staple strands (7249). Each nucleotide carries the charge of one electron and thereby the total charge of the DNA origami structure is: $-14498 \cdot 1.60217662 \cdot 10^{-15} C \; = \; \mathbf{-2.32284 \cdot 10^{-15} C}$

The outer frame of the DNA origami has sides (s) of 120 nm while the inner frame is 40 nm. The area of an equilateral triangle is $\sqrt{3}/4 \cdot s^2$. The total area counting both front- and backside is therefore: $2\left(\sqrt{3}/4 \cdot (120\,nm)^2 - \sqrt{3}/4 \cdot (40\,nm)^2\right) = \mathbf{11085\ nm^2}$

The SCD is therefore: $\mathbf{-2.32284 \cdot 10^{-15} C / 11085\ nm^2}$ = **-209.55** $\boldsymbol{mC/m^2}$

Supplementary methods 1

APTES functionalized mica surfaces were prepared by vapor-phase silanization. 20 ul of (3-Aminopropyl)triethoxysilane) (Sigma-Aldrich, USA) was added to an eppendorf tube, which was placed in a 4 L glass desiccator. Freshly cleaved muscovite mica was placed in the glass desiccator as well. The glass desiccator was flushed with N_2 multiple times and vacuumized for 30 min yielding smooth APTES-mica surfaces.